Journal of Petroleum Science and Engineering 214 (2022) 110487

Contents lists available at ScienceDirect

Journal of Petroleum Science and Engineering

journal homepage: www.elsevier.com/locate/petrol

The effect of surfactant partition coefficient and interfacial tension on oil displacement in low-tension polymer flooding

Kwang Hoon Baek, Mingyan Liu, Francisco J. Argüelles-Vivas, Gayan A. Abeykoon, Ryosuke Okuno *

Hildebrand Department of Petroleum and Geosystems Engineering, The University of Texas at Austin, 200 E. Dean Keeton Street, Stop C0300, Austin, TX, 78712, USA

ARTICLE INFO

Keywords:
Non-ionic surfactant
Short-hydrophobe surfactant
Partition coefficient
Interfacial tension
Polymer flooding

ABSTRACT

This paper presents an experimental study of low-tension polymer (LTP) flooding with a short-hydrophobe surfactant as a sole additive. Such a simple surfactant makes low-tension displacement fronts in polymer flooding (e.g., 10^{-2} mN/m) without involving micro-emulsions of ultra-low interfacial tension (IFT). The envisioned application of LTP flooding is to enhance the displacement of a continuous oil phase with such a moderate reduction in IFT as an effective improvement of polymer flooding.

In our previous research, 2-ethylhexanol-7PO-15EO (2-EH-7PO-15EO) was selected as an optimal short-hydrophobe surfactant that resulted in the lowest IFT between polymer solution and oil, and achieved the greatest final oil recovery. However, this paper presents the effect of surfactant partition coefficients on the LTP flooding as an additional important factor for surfactant optimization.

A series of LTP floods showed that the IFT primarily affected the final oil recovery when the sandpack was swept sufficiently by LTP. Comparison of two cases with similar IFT values (2-EH-4PO-15EO and 2-EH-7PO-25EO) showed that the surfactant partition coefficient affected the oil recovery through its impact on the surfactant in-situ propagation. The case with 2-EH-7PO-25EO resulted in a greater oil recovery because the surfactant propagated more efficiently with a smaller partition coefficient than 2-EH-4PO-15EO.

Results collectively showed that optimization of 2-EH-xPO-yEO for LTP flooding involves two competing factors. One is to minimize the water/oil IFT for increasing the local oil displacement efficiency, and the other is to minimize the partition coefficient for more efficient in-situ propagation of the surfactant. It is critical to take a balance between these two factors for the surfactant used for LTP flooding. The importance of the surfactant partition coefficient became more obvious when a limited amount of surfactant was injected.

1. Introduction

Chemical enhanced oil recovery (EOR) has been studied and developed for more than 60 years including alkali, surfactant, polymer, alkali-surfactant, and alkali-surfactant-polymer (ASP). The commonly-used surfactants in the conventional chemical EOR have a large-hydrophobe with many moles of ethylene oxide (EO) and propylene oxide (PO). Such large hydrophobes usually come from long carbon chain alcohols, such as tridecyl alcohol, oleyl alcohol, and Guerbet alcohols. Certain numbers of moles of EO and PO are attached by an alkoxylation reaction.

Recently, short alcohols and their alkoxylation forms have been studied as a co-solvent to improve ASP formulation, also referred as alkali-cosolvent-polymer flooding (Aitkulov et al., 2017; Fortenberry et al., 2015; Sharma et al., 2018; Upamali et al., 2018). Such co-solvent chemicals were used to promote micro-emulsion phase behavior. For example, the use of alkoxylated short alcohols (isobutyl alcohol, phenol, and 2-ethylhexanol) resulted in micro-emulsion phase behavior with shorter equilibrium time, smaller micro-emulsion viscosity, and less surfactant retention (Upamali et al., 2018). By decreasing the micro-emulsion viscosity and achieving an ultra-low IFT, alkoxylated short alcohols improved oil recovery successfully with a reduced chemical usage (Ghosh et al., 2018; Panthi et al., 2019).

These previous studies on surfactant and co-solvent formulations aimed to achieve a Winsor type III micro-emulsion with ultra-low IFT (e.g., 10^{-3} mN/m). Because multiple chemicals are often required for such an optimal formulation, the chemical cost could be an issue for their field applications. Therefore, Baek et al. (2019 and 2020) evaluated

* Corresponding author.
E-mail address: okuno@utexas.edu (R. Okuno).

https://doi.org/10.1016/j.petrol.2022.110487
Received 22 December 2021; Received in revised form 2 April 2022; Accepted 5 April 2022
Available online 9 April 2022

alkoxylated short alcohols as a single additive to polymer flooding. They referred to it as low-tension polymer (LTP) flooding after the previous studies of using a surfactant in polymer flooding in the 1990s (Kalpakci et al., 1990; Maldal et al., 1998). LTP flooding was a precursor instrumental to the technological advancements that led to the current practice of SP and ASP flooding, such as new surfactants, their formulations, and salinity gradient. The LTP flooding concept was revisited with a new type of surfactants (i.e., short-hydrophobe surfactants) by Baek et al. (2019, 2020).

This research was motivated by a question as to whether there would be a simple modification to polymer flooding in oil reservoirs for which conventional SP flooding would not be practically suitable. For example, applying the desired salinity gradient for ultra-low IFT phase behavior in ASP may be difficult where brine sources are limited for injection into offshore reservoirs. It can be also difficult to handle multiple chemicals because of limited space at the project location (e.g., on an offshore platform). Under these limited conditions, the LTP flooding aims to improve the performance of the polymer flooding by simply adding a short-hydrophobe surfactant in the polymer solution with no other chemicals or additional operation steps.

The major difference between the conventional surfactant-polymer (SP) flooding and the LTP flooding in this research lies in the phase behavior of emulsions. Baek et al. (2020) showed that short-hydrophobe surfactants resulted in a low IFT (e.g., 10^{-2} mN/m with 2-ethylhexanol-7PO-15EO, or 2-EH-7PO-15EO), but not an ultra-low IFT in the order of 10^{-3} mN/m 2-EH-7PO-15EO was found as an optimal short-hydrophobe surfactant by IFT measurements for many short-hydrophobe surfactants. The sandpack flooding of heavy oil achieved a significantly increased oil recovery with 0.5 wt% short-hydrophobe surfactants in the polymer solution, in comparison to polymer flooding. For example, 0.5 wt% 2-EH-7PO-15EO reduced the IFT from 15.8 to 0.025 mN/m, and achieved a recovery factor of 93% the original oil in place (OOIP), in comparison to 66% OOIP with polymer flooding.

As part of the LTP flooding research program, this research was to improve the surfactant optimization method. The central hypothesis was that an optimal surfactant should be determined not only by IFT, but also in terms of surfactant's in-situ distribution during oil displacement, including adsorption on the rock surface, trapping in the remaining oleic phase, and propagation through the aqueous phase.

The in-situ retention of short-hydrophobe surfactants strongly affects the economic feasibility of LTP flooding. The increased oil production should be sufficient to cover the investment in chemical flooding during the operation (Shramm, 2000). Surfactant retention generally includes precipitation, adsorption, and phase trapping. It can determine the success of LTP flooding (Belhaj et al., 2020; Massarweh and Abushaikha, 2020; Shramm, 2000). Precipitation at the reservoir conditions can be avoided by performing a comprehensive stability test of surfactants; therefore, most attention of this research was paid to surfactant adsorption and surfactant trapping in the remaining oil in a sandpack.

At a fixed salinity and temperature above the critical micelle concentration (CMC), surfactant adsorption and its ability to lower the IFT both increase with an increase in relative hydrophobicity of surfactant (Kamal et al., 2017). The degree of adsorption increases and the IFT value decreases as surfactant concentration increases below CMC, and they little change as surfactant concentration increases above CMC (Belhaj et al., 2019; Harwell et al., 1985; Somasundaran and Kunjappu, 1989). By conducting adsorption tests and IFT measurements of 2-EH-x-PO-yEO above CMC, this research aimed to correlate the adsorption with IFT values for 2-EH-xPO-yEO.

Surfactant flooding data showed that an increasing amount of surfactant dissolved in the oleic phase in macro-emulsion retarded the chemical front velocity and delayed the oil recovery (Ding et al., 2020; Hirasaki, 1981; Larson and Hirasaki, 1978). The phase trapping of short-hydrophobe surfactants in the oleic phase can be indicated by a surfactant partition coefficient. The partition coefficient represents the distribution of a surfactant in the oleic and the aqueous phase as the ratio of the surfactant concentration in the oleic phase to that in the aqueous phase, as shown in Equation (1).

$$K = C_S^o / C_S^a \quad (1)$$

where K is the partition coefficient, C_S^o is the surfactant concentration in the oleic phase, and C_S^a is the surfactant concentration in the aqueous phase. It implies the relative affinity of a surfactant for the aqueous phase and for the oleic phase at a certain temperature and pressure (Belhaj et al., 2019; Catanoiu et al., 2011; Ravera et al., 1997). Hence, it indicates the phase trapping behavior of short-hydrophobe surfactants, which affects the surfactant propagation and distribution.

The main objective of this research is to evaluate the performance of short-hydrophobe surfactants with IFT, surfactant distribution, and oil recovery. The surfactant distribution is determined by surfactant adsorption measurement, surfactant partition coefficient, and the overall surfactant balance during LTP flooding. The effect of IFT on the surfactant partition coefficient is also described. This paper presents new experimental results of partition coefficients, adsorption data, and sandpack floodings obtained in this research. For a comprehensive analysis and comparisons, however, some experimental data were taken from Baek et al. (2020): the IFTs of 2-EH-4PO-15EO, 2-EH-4PO-25EO, and 2-EH-7PO-15EO; the surfactant adsorption of 2-EH-7PO-15EO; the polymer flooding data; and the LTP flooding results with 2-EH-7PO-15EO. The experimental conditions in this research were set to be the same as these data taken from Baek et al. (2020), including temperature, brine salinity, oil type, polymer type and concentration, surfactant concentration, and sandpack properties.

Section 2 presents the materials and methods of this research. Section 3 displays the results of IFT and partition coefficient measurements, surfactant adsorption test, and sandpack floodings. Section 4 summarizes the conclusions of this research.

2. Materials and experimental procedure

Experimental conditions were set to mimic the operation plan for an offshore reservoir. It is an unconsolidated sand reservoir of heavy oil. The heavy oil sample used in this research was taken from a reservoir close to the target reservoir because the company has not started oil production from the target reservoir. The reservoir brine and injection brine were set based on their operation plan. More information about the heavy oil and the rheology of polymer solution is provided in Baek et al. (2020). All experiments were conducted at 61 °C.

2.1. Reservoir fluid properties

The reservoir brine and the injection brine were the same with a salinity of 56456 ppm (Table 1). The density of the brine was 1.08 g/ml at 25 °C and 1.05 g/ml at 61 °C. The brine prepared for the experiment contained NaCl (BP358, Fisher Bioreagents), $MgCl_2{\cdot}6H_2O$ (M33, Fisher Chemical), $CaCl_2{\cdot}2H2O$ (C614, Fisher Scientific), KCl (P217, Fisher Chemical), and Na_2SO_4 (S421, Fisher Chemical).

The heavy oil API gravity was 10.8° with a molecular weight of 428 g/ml and a viscosity of 500 cp at 61 °C. The oil density was 0.99 g/ml at

Table 1
Brine composition.

Ions	Concentration [mg/L]
Na^+	18387
K^+	200
Ca^{2+}	2015
Mg^{2+}	958
Cl^-	34883
SO_4^{2-}	13
Total Dissolved Solids	56456

25 °C and 0.95 g/ml at 61 °C. Based on the solubility analysis, the heavy oil sample contained 53.5 wt% saturates, 22.8 wt% aromatics, 20.8 wt% resins, and 2.9 wt% asphaltenes (n-pentane insoluble). The total acid number was 8.08 mg-KOH/g-oil.

2-Ethylhexanol with a certain mole (x and y) of propylene oxide and ethylene oxide (2-EH-xPO-yEO) was applied as a short-hydrophobe surfactant in this research. All surfactants were provided by Harcros Chemicals. Propylene oxide (PO) is related to the hydrophobicity, while ethylene oxide (EO) to the hydrophilicity of the surfactant. The mole numbers of PO and EO substantially affect the surfactant partition coefficient and the IFT as will be shown later. Fig. 1 shows the chemical structure of 2-EH-xPO-yEO. In total, four 2-EH-xPO-yEO surfactants were tested in this research: 2-EH-7PO-15EO, 2-EH-7PO-25EO, 2-EH-4PO-15EO, 2-EH-7PO-25EO.

Partially-hydrolyzed polyacrylamide (HPAM) polymer, Flopaam 3630 (SNF), was selected as the water-soluble polymer. It is a powder-type polymer with a high molecular weight of 20 million Dalton. The surfactant and polymer solution (SP solution) for LTP flooding contained 0.5 wt% surfactant and 0.54 wt% polymer in the reservoir brine, which had a density of 1.04 g/ml at 25 °C and 1.02 g/ml at 61 °C.

2.2. Sandpack

For sandpack preparation, Ottawa sand was filtered into five grain-size categories to match the grain size distribution of the target reservoir (unconsolidated sand) as shown in Table 2. Then, the filtered sand was acidized using 10 wt% HCl solution (2.7 M HCl, pH = −0.44) and dried. The sandpack dimensions were 31-cm in length and 2.58-cm in diameter. The sandpack container was made of transparent polycarbonate, which can be operated at temperatures up to 121 °C. The maximum pressure of the sandpack container was 400 psi with a 1.9-cm wall-thickness.

A new sandpack was prepared for each surfactant adsorption test and each oil recovery experiment. Each sandpack was prepared by following the same procedure. The weight of sandpack for each LTP flooding ranged from 350 g to 365 g. The porosity and the permeability of each sandpack is summarized in Table 7.

2.3. IFT measurement

The water/oil IFT of four surfactant samples (2-EH-7PO-15EO, 2-EH-7PO-25EO, 2-EH-4PO-15EO, and 2-EH-4PO-25EO) were measured by a spinning drop method (KRÜSS tensiometer) at 61 °C. The aqueous solution of each sample contained 1.0 wt% surfactant in the reservoir brine. The IFT results were taken from Baek et al. (2020). The CMC of 2-EH-7PO-15EO was measured to be 0.025 wt%. Therefore, we assumed that CMC values of other 2-EH-xPO-yEO surfactants were significantly smaller than the tested concentrations, e.g., 0.5 wt% (LTP flooding) and 1.0 wt% (IFT measurement).

2.4. Partition coefficient measurement

Samples were prepared in a 20-ml glass vial. The equal volume (4 mL) of the heavy oil and the aqueous solution were added to the glass vial using a repeater. The aqueous phase was the reservoir brine with a certain concentration (0.1 wt%, 0.2 wt%, 0.3 wt%, 0.4 wt%, 0.5 wt%, and 1.0 wt%) of short-hydrophobe surfactants (2-EH-7PO-15EO, 2-EH-7PO-25EO, 2-EH-4PO-15EO, and 2-EH-4PO-25EO).

One trial included six samples with six different concentrations of a surfactant. Each trial was repeated three times, which resulted in 18 samples in total. Three sets of samples were kept in an oven at 61 °C for 30 min, and then all samples were mixed using a vortex mixer. Then, all samples were kept in an oven at 61 °C for five days. In the first two days, each sample was mixed eight times per day. Samples were then aged at the target temperature (61 °C and 25 °C) for additional six days.

The amount of a surfactant in the aqueous phase at equilibrium was measured by high-performance liquid chromatography (HPLC). Samples were kept at their respective temperature, and the aqueous phase from each sample was extracted by using a disposable needle and a disposable syringe. Then, each aqueous phase was diluted by deionized water with a dilution factor of four. The dilution factor may vary from 2 to 10 depending on the HPLC peak limit. The concentration of the surfactant in the aqueous phase was then measured by HPLC. The amount of the surfactant in the oleic phase was calculated based on material balance.

Table 2
Grain size distribution of sandpack.

Sieve Number	Lower Limit (μm)	Upper Limit (μm)	Average Size (μm)	Mass Concentration (%)
325	45	105	75	20
140	105	150	127.5	18
100	150	210	180	29
70	210	420	315	28
40	420	710	565	5

2.5. SP solution and polymer solution preparation

The concentrations of HPAM 3630s polymer and each short-hydrophobe surfactant were set to be the same as Baek et al. (2020). The polymer concentration in the injection brine was 0.54 wt% to match 60 cp at the shear rate of 7 s^{-1} at 61 °C (i.e., the viscosity ratio with the 500-cp oil was approximately 8). For surfactant-polymer (SP) solutions, 0.5 wt% of a short-hydrophobe surfactant was added to the polymer solution. The surfactant concentration was set to sufficiently overcome the surfactant adsorption and trapping in the remaining oleic phase so that the surfactant could propagate through the sandpack to be detected from the effluent samples. In addition, insufficient surfactant propagation was tested by using 0.1 wt% surfactant in the polymer solution as will be discussed later.

Since HPAM 3630s is a power-type polymer, special care is required to make polymer and SP solutions. Before adding the polymer powder, each batch solution was mixed under 500 rpm. Then, the polymer powder was slowly and continuously added to each batch to avoid polymer aggregation and degradation. Each batch solution was less than 400 ml. After the polymer addition, each batch was mixed under 500 rpm for 3 h. After the mixing, the solution was filtered using a 1.2 μm

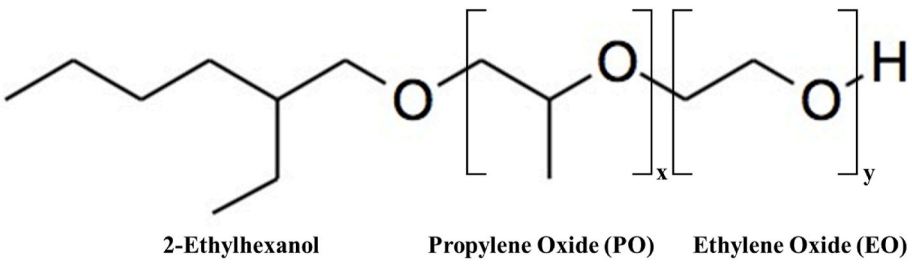

Fig. 1. The chemical structure of 2-EH-xPO-yEO.

filter under 15 psi argon gas. By recording the time duration to collect each 20 ml solution, the filtration ratio (FR) was calculated to confirm the homogeneity of the polymer solution. FR is the time duration to collect 60 ml–80 ml solution divided by the time duration to collect 180 ml–200 ml solution. FR should be between 1.0 and 1.2. After filtration, the solution was stirred at 350 rpm and was degassed with argon gas for 30–60 min at the same time to eliminate oxygen in the sample solution. The prepared solutions were immediately transferred into accumulators for the subsequent experiments. If the solutions were not used immediately, they should be kept in the refrigerator under 10 °C for 2 day at most, which is not the case for this research.

2.6. LTP flooding

Unlike the ASP flooding that aims to achieve an ultra-low IFT (i.e., 10^{-3} mN/m) through Winsor type III emulsion phase behavior, the LTP flooding with a short-hydrophobe surfactant expects a moderate reduction of the water/oil IFT. Therefore, the LTP flooding is more applicable for displacing a continuous oil phase rather than dispersed oil droplets trapped after waterflooding. For all cases, therefore, the LTP flooding was performed as the secondary mode without a prior waterflood.

Fig. 2 displays the experimental set-up for the LTP flooding. The experimental temperature was 61 °C; therefore, all equipment was placed inside an oven (Blue M). Four accumulators were prepared for heavy oil, brine, SP solution, and polymer solution. The bottom of each accumulator was filled with deionized water and connected to ISCO pumps. The fluid accumulators were pressure-controlled by pumps, or controlled by a constant flow rate when a specific fluid was injected. All lines were purged with deionized water or injection fluids to remove any possible air in the system. A pressure transducer (OMEGA) was installed to measure the inlet pressure. The pressure difference between the inlet and the outlet of the sandpack was measured by a differential pressure flow transmitter (Rosemount). The inlet pressure and the pressure difference were recorded in a data requisition system (LabView).

After setting up accumulators and the sandpack, the system was left in a Blue M oven at 61 °C for a day to achieve temperature equilibrium for all equipment and fluids. After confirming the stable system temperature at 61 °C, the sandpack was evacuated for 2 h. Then, the sandpack was first saturated with brine to measure the pore volume of the sandpack. After measuring the pore volume, the brine was injected at different flow rates to measure the permeability using Darcy's law. The 200-ml of heavy oil was then injected into the sandpack for 20 h at 10 ml/h for oil saturation. While injecting oil, effluents were collected to calculate the initial oil and water saturations in the sandpack. When the sandpack was ready (i.e., known S_{oi}, S_{wi}, porosity, and permeability), the SP solution was injected to conduct the LTP flooding.

A total of five LTP floodings were conducted: (1) 0.5 wt% 2-EH-7PO-15EO, (2) 0.5 wt% 2-EH-7PO-25EO, (3) 0.5 wt% 2-EH-4PO-15EO, (4) 0.1 wt% 2-EH-7PO-25EO, and (5) 0.1 wt% 2-EH-7PO-15EO. For each case, 0.5 pore volume (PV) of the SP solution was injected at a constant flow rate of 1 ml/h. Then, 4.5 PV of polymer solution was injected after the SP injection at a constant flow rate of 3 ml/h. Effluent samples were collected for every 6 ml–9 ml. HPLC was used to measure the surfactant amount in the aqueous phase of effluents.

2.7. Surfactant adsorption test

This was a dynamic adsorption test for a short-hydrophobe surfactant on sand grains. The experimental set-up was the same as the LTP flooding (Fig. 2). After saturating the sandpack with the reservoir brine, 0.5 PV of the SP solution (0.5 wt% surfactant and 0.54 wt% polymer in the reservoir brine) was injected at a constant flow rate of 9 ml/h. Then, the polymer solution (0.54 wt% polymer in the reservoir brine) was injected for 2.5 PV at a constant flow rate of 9 ml/h. Effluent samples were collected for every 5 ml. The short-hydrophobe surfactant concentration in each aqueous phase was analyzed by HPLC.

3. Results and discussion

3.1. IFT

Table 3 presents the IFT data obtained for 1.0-wt% short-hydrophobe surfactant solutions at a salinity of 56456 ppm with the heavy oil at 61 °C. The four surfactants were compared to understand the impact of

Table 3
IFT results for 1.0 wt% surfactant in the 56456-ppm brine with heavy oil at 61 °C.

Short-hydrophobe Surfactant	IFT (mN/m)
2-EH-4PO-15EO	0.20
2-EH-4PO-25EO	0.87
2-EH-7PO-15EO	0.025
2-EH-7PO-25EO	0.18

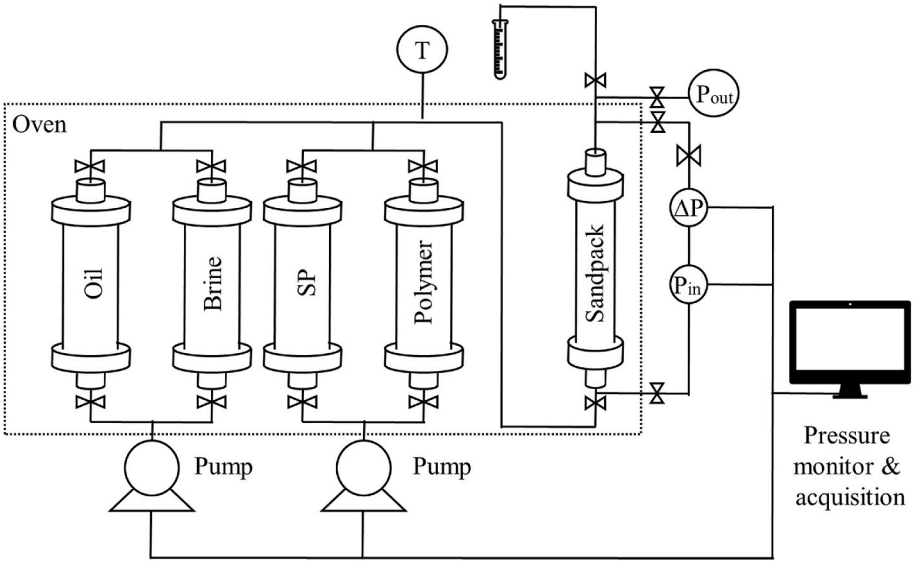

Fig. 2. Experiment set-up for the sandpack flooding and adsorption test.

PO (EO) on the IFT while keeping the EO (PO) number. 2-EH-7PO-15EO resulted in the smallest IFT, 0.025 mN/m, among the four short-hydrophobe surfactants. The IFT was increased to approximately 0.2 mN/m by decreasing the PO number to 4 while keeping the EO number (2-EH-4PO-15EO), or by increasing the EO number to 25 while keeping the PO number (2-EH-7PO-25EO). The adverse effects of decreasing the PO number and increasing the EO number on the IFT resulted in 0.87 mN/m with 2-EH-4PO-25EO.

3.2. Partition coefficient

Table 4 summarizes the partition coefficient data for short-hydrophobe surfactants with different initial concentrations in the aqueous phase at 25 °C and 61 °C. Each measurement was repeated at least three times. The LTP flooding was performed at 61 °C; therefore, the partition coefficient at 61 °C was used to calculate the trapped surfactant in the remaining oil. Surfactant concentrations in effluent samples from the LTP flooding were calculated with the partition coefficients at 25 °C.

For all measurements, the concentration of short-hydrophobe surfactants was significantly greater than its CMC; therefore, only the post-CMC regime is discussed. We considered the effects of temperature and the initial surfactant concentration. Results are shown in Fig. 3 for 25 °C and Fig. 4 for 61 °C. The partition coefficient decreased with increasing initial surfactant concentration. At 61 °C, for example, the partition coefficients at 0.5 wt% and 1.0 wt% 2-EH-4PO-15EO were 1.61 and 0.90, respectively. Also, the partition coefficient increased with increasing temperature for a given concentration. For 0.5 wt% 2-EH-4PO-15EO, the partition coefficient increased from 1.08 to 1.61 as the temperature increased from 25 °C to 61 °C.

The effect of temperature on the partition coefficient was explained by the standard free energy of partitioning; that is, the difference in chemical potentials of the surfactant when it is in the oleic phase and in the aqueous phase (Ghoulam et al., 2002; Salager et al., 2000). Note that the definition of the partition coefficient was reversed in their research (i.e., the surfactant concentration in the aqueous phase over that in the oleic phase). As temperature increases, the standard free energy of partitioning decreases, resulting in more surfactant in the oleic phase. They explained that this behavior is similar to the aqueous solubility of surfactant decreasing with increasing temperature, resulting in the transfer of more surfactant to the oleic phase.

Table 4
Surfactant partition coefficient (the average of three repeated measurements). The initial surfactant concentration in the aqueous phase was fixed for each sample. The surfactant concentration in the aqueous phase was measured by HPLC, and the surfactant concentration in the oleic phase was calculated based on the material balance.

Surfactant	25 °C		61 °C	
	Initial surf. conc. in aq. phase (wt%)	Partition coefficient	Initial surf. conc. in aq. phase (wt%)	Partition coefficient
2-EH-4PO-15EO	0.1	2.23	0.1	2.75
	0.2	1.56	0.2	2.43
	0.3	1.33	0.3	2.26
	0.4	1.21	0.4	1.93
	0.5	1.08	0.5	1.61
	1.0	0.70	1.0	0.90
2-EH-4PO-25EO	0.1	0.28	0.1	0.53
	0.2	0.22	0.2	0.45
	0.3	0.20	0.3	0.36
	0.4	0.17	0.4	0.28
	0.5	0.31	0.5	0.22
	1.0	0.07	1.0	0.10
2-EH-7PO-15EO	0.1	4.43	0.1	4.57
	0.2	2.51	0.2	3.14
	0.3	2.00	0.3	2.41
	0.4	1.66	0.4	2.25
	0.5	1.73	0.5	1.93
	1.0	0.95	1.0	1.10
2-EH-7PO-25EO	0.1	1.25	0.1	1.82
	0.2	1.03	0.2	1.42
	0.3	0.80	0.3	1.09
	0.4	0.78	0.4	0.90
	0.5	0.63	0.5	0.68
	1.0	0.41	1.0	0.45

Regarding the effect of surfactant concentration on the partition coefficient, a similar partition coefficient behavior was observed by Belhaj et al. (2019), who measured the partition coefficient of a non-ionic surfactant, alkylpolyglucoside. The partition coefficient of alkylpolyglucoside decreased with increasing surfactant concentration when surfactant concentrations were above the CMC. They explained that, above the CMC, a surfactant is no longer consumed by creating micelles that go to the oil/water interface. As a result, more surfactants remain in the aqueous phase, and the partition coefficient decreases.

Another possible explanation is specific to the brine used, which contained divalent cations at approximately 3000 ppm (Ca^{2+} and Mg^{2+} in Table 1). These divalent cations can interact with the PO and EO groups of the surfactant used, causing it to be less soluble in the aqueous phase. In fact, Boss and Mott (1980) and Maltesh and Somasundaran (1992) showed that divalent cations bind to polyethylene glycol (PEG), which contains multiple EO groups. This effect of divalent cations tends to diminish with an increasing number of moles of PO and EO groups with increasing initial concentration of the surfactant in the solution. This effect of divalent cations on increasing the partition coefficient may be enhanced by temperature because the hydrophilicity of the surfactant tends to become weaker with higher temperature, resulting in more interaction with divalent cations. This additional question warrants further investigation with more experiments, but it is beyond the scope of this paper.

3.3. Surfactant adsorption

Table 5 and Fig. 5 show the short-hydrophobe surfactant concentration in the aqueous phase at the effluent in the adsorption test. The surfactant adsorption for each surfactant was calculated by the mass balance among an injected surfactant amount, a recovered surfactant amount, and a total sand mass. The unrecovered amount of surfactant was considered as the adsorption on sand grains. Note that there was no oleic phase in the surfactant adsorption measurement. The adsorptions of 2-EH-4PO-15EO, 2-EH-7PO-15EO, and 2-EH-7PO-25EO were 0.019 mg/g-sand, 0.055 mg/g-sand, and 0.020 mg/g-sand, respectively. All adsorption results were relatively small (e.g., < 0.1 mg/g-rock), indicating the technical feasibility as an additive for LTP flooding.

The breakthrough times of 2-EH-4PO-15EO and 2-EH-7PO-25EO were similar at 1.05 PVI and 1.02 PVI, respectively. However, a delayed breakthrough (1.13 PVI) was observed with 2-EH-7PO-15EO. This difference likely comes from the larger adsorption amount (0.055 mg/g) of 2-EH-7PO-15EO, which is 2.8 times larger than the other two surfactants (0.020 mg/g). A larger amount of adsorption causes surfactant retardation and results in a delayed breakthrough. Note that there was no oleic phase in the adsorption test; hence, the partition coefficient was not a factor affecting the surfactant concentration in effluents.

The lowest adsorption value of 2-EH-4PO-15EO is likely related to the shortest carbon chain. However, 2-EH-7PO-25EO which has the longest carbon chain resulted in lower adsorption compared to 2-EH-7PO-15EO. That is, for these three short-hydrophobe surfactants, a negative correlation was observed between the IFT and the adsorption.

The surfactant adsorption is a complex mechanism involving many different factors, such as surfactant types and concentrations, rock types, clays, temperature, and brine salinity and composition. For example, the adsorption of non-ionic surfactant on silica depended on its concentration (Tiberg et al., 1994). Below the critical micelle concentration (CMC), the non-ionic surfactant adsorption increased with increasing

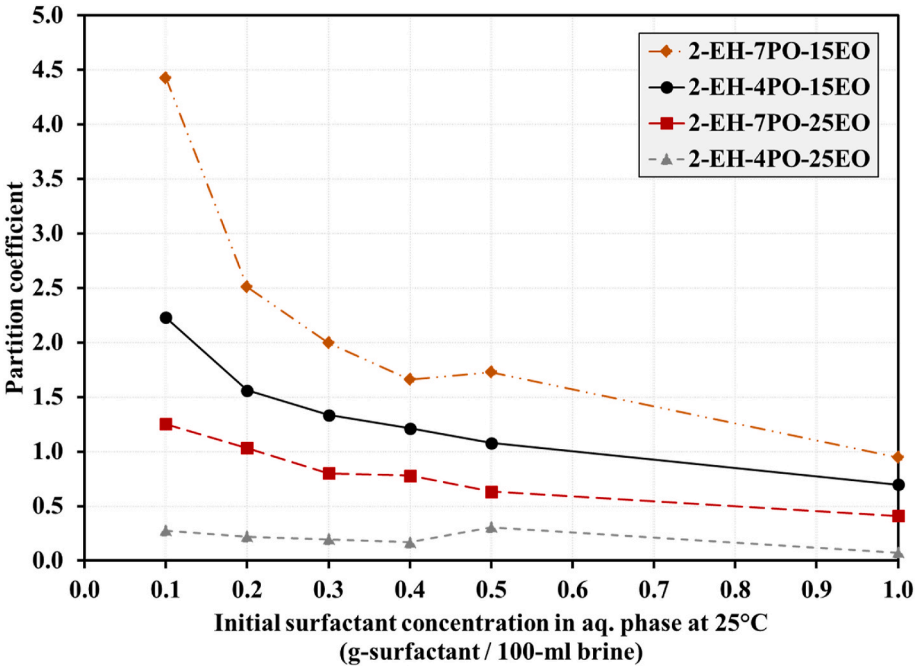

Fig. 3. Partition coefficients of 2-EH-xPO-yEO at 25 °C. The oil/aqueous system contained an equal amount of oil phase and aqueous phase. The brine salinity was 56456 ppm. Each point shows a partition coefficient of short-hydrophobe surfactants (2-EH-7PO-15EO, 2-EH-7PO-25EO, 2-EH-4PO-15EO, and 2-EH-4PO-25EO) with different initial concentrations (0.1 wt%, 0.2 wt%, 0.3 wt%, 0.4 wt%, 0.5 wt%, and 1.0 wt%).

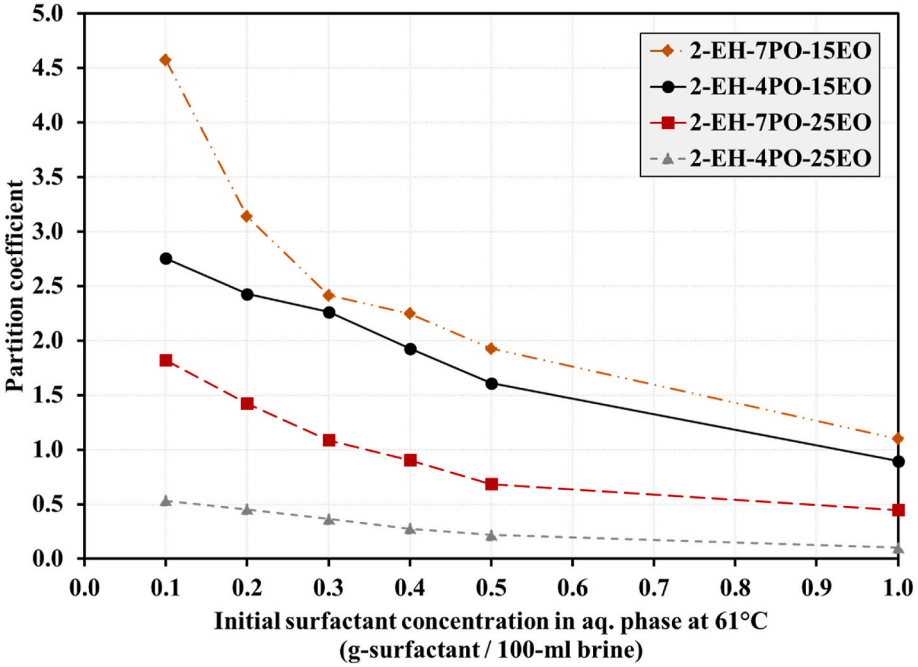

Fig. 4. Partition coefficients of 2-EH-xPO-yEO at 61 °C. The oil/aqueous system contained an equal amount of oil phase and aqueous phase. The brine salinity was 56456 ppm. Each point shows a partition coefficient of short-hydrophobe surfactants (2-EH-7PO-15EO, 2-EH-7PO-25EO, 2-EH-4PO-15EO, and 2-EH-4PO-25EO) with different initial concentrations (0.1 wt%, 0.2 wt%, 0.3 wt%, 0.4 wt%, 0.5 wt%, and 1.0 wt%).

surfactant concentration. Above the CMC, the adsorption of non-ionic surfactants remained the same.

Two fundamental interactions affect the surfactant adsorption (Rupprecht and Gu, 1991). Electrostatic interaction involves the charge of surfactant ions, the charge of rock surfaces, and pH. For example, anionic surfactants resulted in less adsorption on silica or sandstones that have a negative surface charge (Mannhardt et al., 1992). The short-hydrophobe surfactants in this research are non-ionic. For non-ionic surfactants, the hydrophobic interaction between the hydrophobic group of the surfactant and the rock surface can be the main adsorption mechanism (Kamal et al., 2017; Rupprecht and Gu, 1991). That is, a larger amount of surfactant adsorption is expected with more hydrophobic surfactants.

The hydrophobicity of 2-EH-xPO-yEO depends on the PO group and the EO group. In general, the PO group increases hydrophobicity and also decreases the IFT between the surfactant solution and oil. On the

Table 5
Results of adsorption tests for 2-EH-4PO-15EO, 2-EH-7PO-15EO, and 2-EH-7PO-25EO. The total amount of surfactant injection was calculated based on the total SP injected volume. The surfactant concentration in each effluent was measured by HPLC. The adsorption (the bottom row) was calculated based on the loss divided by the mass of the sandpack.

	2-EH-4PO-15EO	2-EH-7PO-15EO	2-EH-7PO-25EO
Total surfactant injection (g)	0.168	0.178	0.173
Recovered surfactant (g)	0.161	0.158	0.166
Surfactant loss (g)	0.007	0.020	0.007
Sandpack mass (g)	354.7	360.5	350.3
Adsorption (mg/g-sandpack)	0.019	0.055	0.020

other hand, the EO group decreases hydrophobicity and increases the IFT. The negative correlation between the IFT and the adsorption can be explained by the hydrophobic interaction. That is, the stronger hydrophobicity of 2-EH-xPO-yEO as non-ionic surfactants causes the IFT to decrease, and also more adsorption on the silica surfaces. Indeed, 2-EH-7PO-15EO had the strongest hydrophobicity among the surfactants tested, and therefore it gave the largest adsorption and the smallest IFT value.

In terms of surface adsorption, 2-EH-4PO-15EO and 2-EH-7PO-25EO are more favorable than 2-EH-7PO-15EO; however, 2-EH-4PO-15EO and 2-EH-7PO-25EO give IFTs that are one order of magnitude greater than 2-EH-7PO-15EO. In the next section, these three short-hydrophobe surfactants are compared in oil displacement efficiency.

3.4. LTP flooding results

Based on the IFT and surfactant adsorption results, three surfactants were selected for the oil recovery experiment: 2-EH-4PO-15EO, 2-EH-7PO-15EO, and 2-EH-7PO-25EO. The effect of partition coefficients with the same IFT can be compared between 2-EH-4PO-15EO and 2-EH-7PO-25EO. The effect of partition coefficients with different IFTs can be compared between 2-EH-7PO-15EO and 2-EH-7PO-25EO. 2-EH-4PO-25EO was not included in the oil recovery experiment because of the high IFT value.

Table 6 and Table 7 summarize the experimental conditions for five LTP floods. For Floods #1 - #3, the slug was 0.5-wt% surfactant for 0.5 pore volume injection (PVI). These cases were designed for the low-tension displacement front to break through with a sufficient amount of surfactant. Floods #4 and #5 were designed to represent a slug with a limited amount of surfactant, with which the adverse effects of surfactant's adsorption and trapping in oil would be more significant on oil recovery. The amount of surfactant in Floods #4 and #5 was five times smaller than that in the other cases.

All results are summarized Table 8, Table 9, and Figs. 6–12. Table 8 gives oil recovery data for the five LTP floods. Figs. 6–8 present the profiles of oil recovery and surfactant concentration in the aqueous phase of the effluent samples for Floods #1 - #3. Fig. 9 compares three LTP floods. Fig. 10 and Fig. 11 show the results for Floods #4 and #5. Finally, Fig. 12 summarized data from all five LTP floods and the polymer flood as a control experiment. Results of the polymer flood, Flood #2, and Flood #5 with 2-EH-7PO-15EO were taken from Baek et al. (2020).

Flood #2 (2-EH-7PO-15EO) achieved the highest oil recovery of 93% at 5 PVI, which was 19% higher than Flood #1 (2-EH-4PO-15EO) and 9% higher than Flood #3 (2-EH-7PO-25EO). The oil recovery factors at the early stage before 1.0 PVI were similar to one another among Flood #1, #2, and #3 with a difference of 3–5%. The difference in oil recovery factor became larger after 1.5 PVI.

The highest oil recovery for Flood #3 was attributed to the IFT

Table 6
LTP flooding conditions.

Temperature		61 °C
Porous medium		Ottawa sand
Brine salinity (reservoir brine = injection brine)		56456 ppm
Viscosity (61°C)	Oil	500 cP
	Polymer solution (at the shear rate of 7 sec^{-1})	60 cP
	SP solution (at the shear rate of 7 sec^{-1})	60 cP

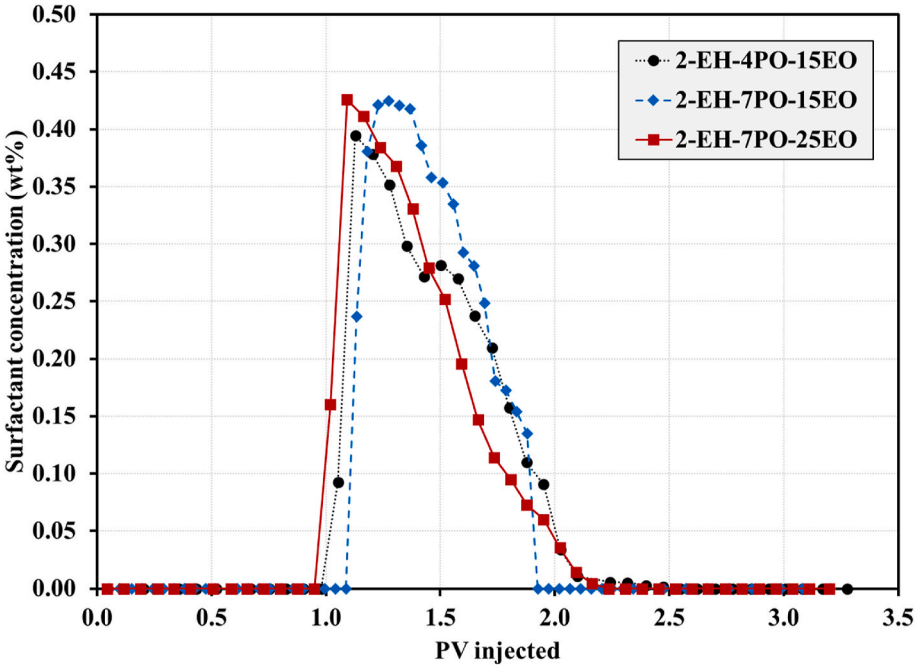

Fig. 5. 2-EH-xPO-yEO concentrations in effluents of adsorption tests. The short-hydrophobe surfactant concentration in each effluent was measured by HPLC. The injected and produced amounts were 0.168 g and 0.161 g for 2-EH-4PO-15EO, 0.178 g and 0.158 g for 2-EH-7PO-15EO, and 0.173 g and 0.166 g for 2-EH-7PO-25EO.

Table 7
LTP flooding summary.

Experiment	LTP Flooding	LTP Flooding	LTP Flooding	LTP Flooding	LTP Flooding
	Flood #1	Flood #2	Flood #3	Flood #4	Flood #5
Porosity	34%	33%	35%	35%	35%
Permeability	9.3 Darcy	9.3 Darcy	9.6 Darcy	9.3 Darcy	9.6 Darcy
Pore volume	64.5 mL	64.4 mL	68.2 mL	67.8 mL	66.5 mL
S_{oi}	89%	84%	87%	85%	85%
S_{wi}	11%	16%	13%	15%	15%
Surfactant	2-EH-4PO-15EO	2-EH-7PO-15EO	2-EH-7PO-25EO	2-EH-7PO-25EO	2-EH-7PO-15EO
Polymer	HAPM 3630s	HAPM 3630s	HAPM 3630s	HAPM 3630s	HAPM 3630s
LTP slug	0.5 PVI 0.5 wt% surfactant 0.54 wt% polymer 56456 ppm brine	0.5 PVI 0.5 wt% surfactant 0.54 wt% polymer 56456 ppm brine	0.5 PVI 0.5 wt% surfactant 0.54 wt% polymer 56456 ppm brine	0.5 PVI 0.1 wt% surfactant 0.54 wt% polymer 56456 ppm brine	0.5 PVI 0.1 wt% surfactant 0.54 wt% polymer 56456 ppm brine
Chase polymer	4.5 PVI 0.54 wt% polymer 56456 ppm brine	4.5 PVI 0.54 wt% polymer 56456 ppm brine	4.5 PVI 0.54 wt% polymer 56456 ppm brine	4.5 PVI 0.54 wt% polymer 56456 ppm brine	4.5 PVI 0.54 wt% polymer 56456 ppm brine

Table 8
Oil recovery summary. The comparison is also shown in Fig. 12.

PVI	Oil Recovery (%OOIP)				
	Flood#1 0.5 PVI 0.5 wt% 2-EH-4PO-15EO	Flood#2 0.5 PVI 0.5 wt% 2-EH-7PO-15EO	Flood#3 0.5 PVI 0.5 wt% 2-EH-7PO-25EO	Flood#4 0.5PVI 0.1 wt% 2-EH-7PO-25EO	Flood#5 0.5PVI 0.1 wt% 2-EH-7PO-15EO
0.5	47	51	55	46	51
1.0	65	70	67	60	63
1.5	68	78	72	67	68
2.0	71	82	75	71	72
2.5	72	87	77	74	76
3.0	73	89	79	77	78
3.5	73	91	80	78	80
4.0	74	92	82	80	81
4.5	74	93	83	80	82
5.0	74	93	84	81	82

reduction by three orders of magnitude from 15.8 mN/m to 0.025 mN/m with 2-EH-7PO-15EO. The reduced IFT resulted in a delayed polymer breakthrough and a large oil cut until polymer breakthrough. For this experiment setup, the average permeability was 9.5 Darcy, the pressure drop was 0.44 bar/m, and the length of the sandpack was 30.48 cm; therefore, the IFT reduction by 2-EH-7PO-15EO resulted in an increase in the capillary number (N_C) from 2.7×10^{-5} to 1.7×10^{-2}, leading to the observed capillary desaturation.

The IFT was lowered from 15.8 mN/m to 0.20 mN/m and 0.18 mN/m using 2-EH-4PO-15EO (Flood #1) and 2-EH-7PO-25EO (Flood #3), respectively. In comparison to Flood #2, the polymer breakthrough occurred earlier for Floods #1 and #3; therefore, the oil cut curves were relatively smaller for Floods #1 and 3 than for Flood #2. With the same experiment setup, N_C is 2.1×10^{-3} for Flood #1 and 2.3×10^{-3} for Flood #3. That is, they were one order of magnitude smaller than N_C for Flood #2.

Table 9 summarized the surfactant retention results for Floods #1, #2, #3, and #4.2-EH-7PO-25EO (Flood #3) resulted in the least retention among the three surfactants, resulting in a surfactant recovery factor of 86% (in the aqueous and the oleic phases). 2-EH-7PO-15EO (Flood #2) resulted in the largest amount of retention in the remaining oil and on solid surfaces with the surfactant recovery factor of only

Table 9
Surfactant mass balance of Floods #1, #2, #3, and #4. The total amount of surfactant injection was calculated based on the slug injection volume. For effluents, the surfactant concentration in the aqueous phase was measured by HPLC. The surfactant concentration in the oleic phase of the effluents was calculated based on the partition coefficient. The surfactant retention in the sandpack is the summation of the adsorbed surfactant mass and the surfactant trapped in remaining oil calculated by the partition coefficient.

	Flood #1 0.5 PVI 0.5 wt% 2-EH-4PO-15EO	Flood #2 0.5 PVI 0.5 wt% 2-EH-7PO-15EO	Flood #3 0.5 PVI 0.5 wt% 2-EH-7PO-25EO	Flood #4 0.5 PVI 0.1 wt% 2-EH-7PO-25EO
Total surfactant injection (g)	0.1613	0.1610	0.1707	0.0339
Total recovery (effluent) (g)	0.1086 (67.3%)	0.1018 (63.3%)	0.1465 (85.8%)	0.0055 (16.1%)
- Recovery in aqueous phase (g)	0.0986	0.0751	0.1327	0.0049
- Recovery in oleic phase (g)	0.0101	0.0268	0.0138	0.0006
Total retention in sandpack (g)	0.0527 (32.7%)	0.0592 (36.7%)	0.0242 (14.2%)	0.0284 (83.9%)
- Trapped in remaining oil (g)	0.0458	0.0396	0.0171	0.0214
- Adsorption in sandpack (g)	0.0069	0.0196	0.0071	0.0070

63%. 2-EH-4PO-15EO had nearly the same adsorption as 2-EH-7PO-25EO as shown in Table 5; however, 2-EH-4PO-15EO was retained more (Flood #1) than 2-EH-7PO-25EO (Flood #3) because the former left a larger amount of remaining oil (i.e., less efficient oil displacement) as shown in Table 8.

For a field application, the LTP slug would be injected for a shorter time than 5 PVI; therefore, the chemical propagation would be important as it determines the early-time oil recovery. As shown by the surfactant concentrations in Figure 9, 2-EH-7PO-25EO propagated fastest in the highest concentration, whereas 2-EH-4PO-15EO showed a relatively delayed propagation with an extended tail. These results came from the retardation and retention of surfactant via the mass transfer to oil and the surface adsorption (Ding et al., 2020).

The comparison of LTP floods with the same IFT, Flood #1 (2-EH-4PO-15EO) and Flood #3 (2-EH-7PO-25EO), further illustrates the importance of surfactant propagation. 2-EH-4PO-15EO had a greater partition coefficient, leading to a slower propagation of the displacement front. In contrast, 2-EH-7PO-25EO had the smallest partition coefficient and least tendency of partitioning into the oleic phase, leading to efficient propagation of the displacement front. The oil recovery comparison (Fig. 9) shows that a lower partition coefficient with less retardation caused the oil production for Flood # 3 to be consistently greater than that for Flood #1. After 1.5 PVI, the incremental oil recovery for Flood #3 was 5–10% greater than that for Flood #1.

Baek et al. (2020) concluded that the 2-EH-7PO-15EO was an optimum surfactant in terms of oil displacement efficiency. However, the LTP flooding with 2-EH-7PO-15EO and 2-EH-7PO-25EO performed equally well until 1 PVI. Furthermore, the in-situ retention of 2-EH-7PO-15EO was more than twice greater than that of 2-EH-7PO-25EO as shown in Table 5. These results indicate that 2-EH-7PO-25EO would give a greater volumetric sweep efficiency with only slightly less efficient oil displacement than 2-EH-7PO-15EO.

Since the amount of surfactant was reduced by a factor of five for Floods #4 (Fig. 10) and #5 (Fig. 11), their results are more affected by the surfactant propagation before 1.0 PVI. Although their recoveries continued to increase, the early-time oil recovery was clearly less efficient than in Floods #1–3. With this limited SP slug size, the breakthrough times (water and polymer) of Floods #4 and #5 were similar to each other. The oil recovery of Flood #4 after 1.5 PVI remained only 1–2% smaller than that of Flood #5, although the IFT for Flood #5 was

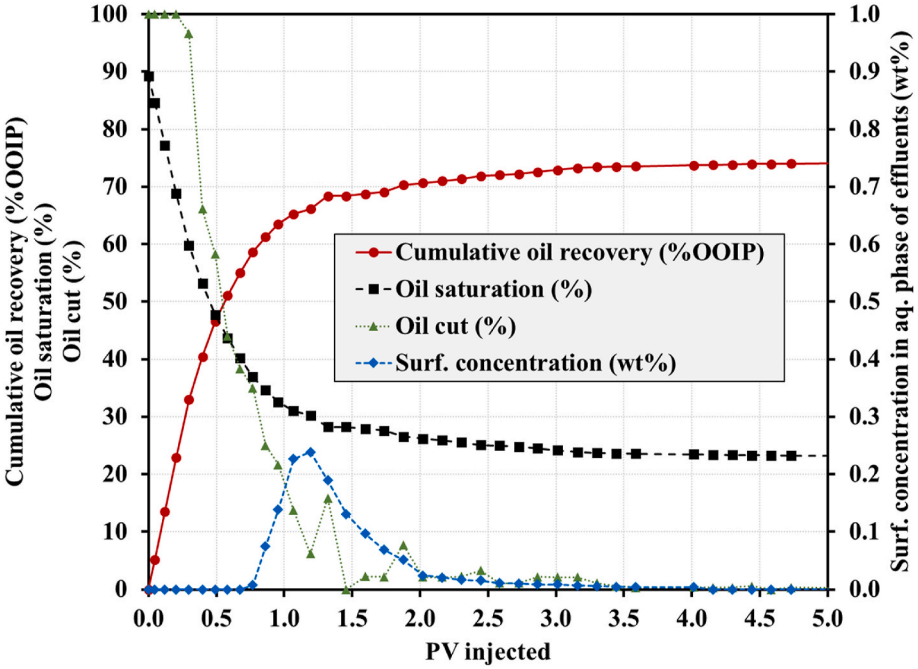

Fig. 6. LTP flooding results with a slug of 0.5 wt% 2-EH-4PO-15EO for 0.5 PVI (Flood #1).

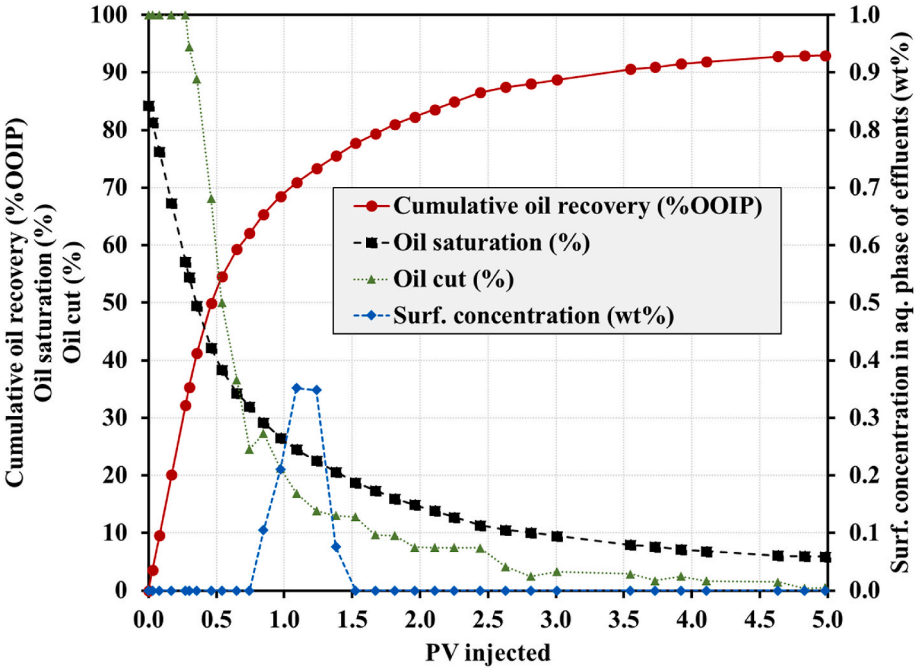

Fig. 7. LTP flooding results with a slug of 0.5 wt% 2-EH-7PO-15EO for 0.5 PVI (Flood #2).

one magnitude smaller than that of Flood #4. The surfactant profiles of the effluent samples in Flood #4 show that 14.5 wt% of 2-EH-7PO-25EO was recovered from the aqueous phase at the effluent. A total of 16.1 wt % of 2-EH-7PO-25EO was recovered from effluent samples, including both the oleic and the aqueous phases. In contrast, there was no recovered 2-EH-7PO-15EO in Flood #5. These results indicate that 2-EH-7PO-25EO had a better propagation than 2-EH-7PO-15EO.

Results collectively show that optimization of 2-EH-xPO-yEO for LTP flooding involves two competing factors. One is to minimize the water/oil IFT for increasing the local oil displacement efficiency, and the other is to minimize the partition coefficient for increasing the volumetric sweep efficiency with more efficient in-situ propagation of the surfactant. Among the short-hydrophobe surfactants studied, 2-EH-7PO-25EO appears to take a balance between the two factors. For field applications, the surfactant concentration should also be optimized based on the project economics. Although this paper is focused on oil-displacement efficiency by low-tension polymer, the polymer viscosity should be adjusted for the reduced IFT by the selected surfactant in order to optimize the volumetric sweep efficiency.

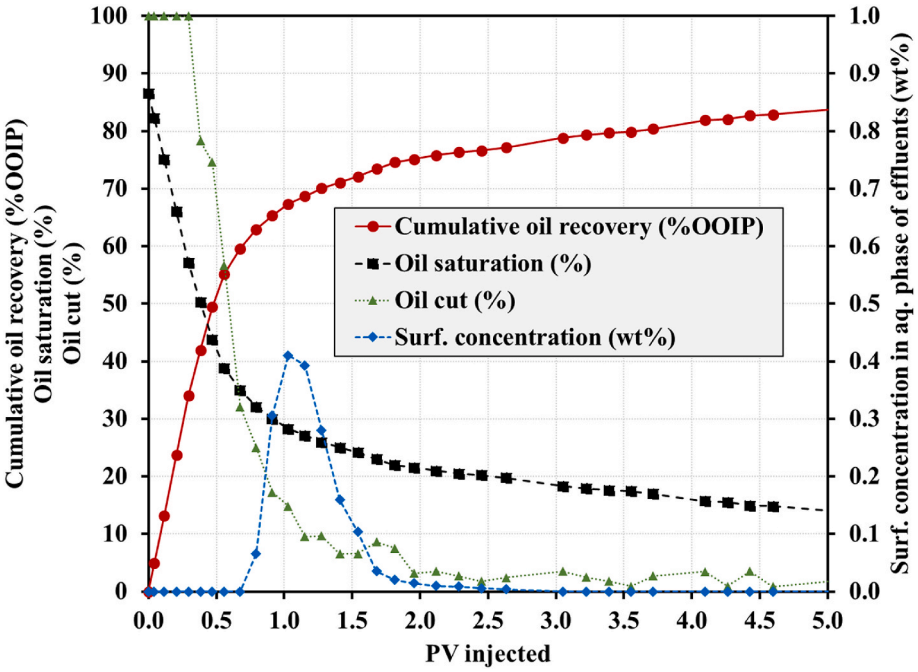

Fig. 8. LTP flooding results with a slug of 0.5 wt% 2-EH-7PO-25EO for 0.5 PVI (Flood #3).

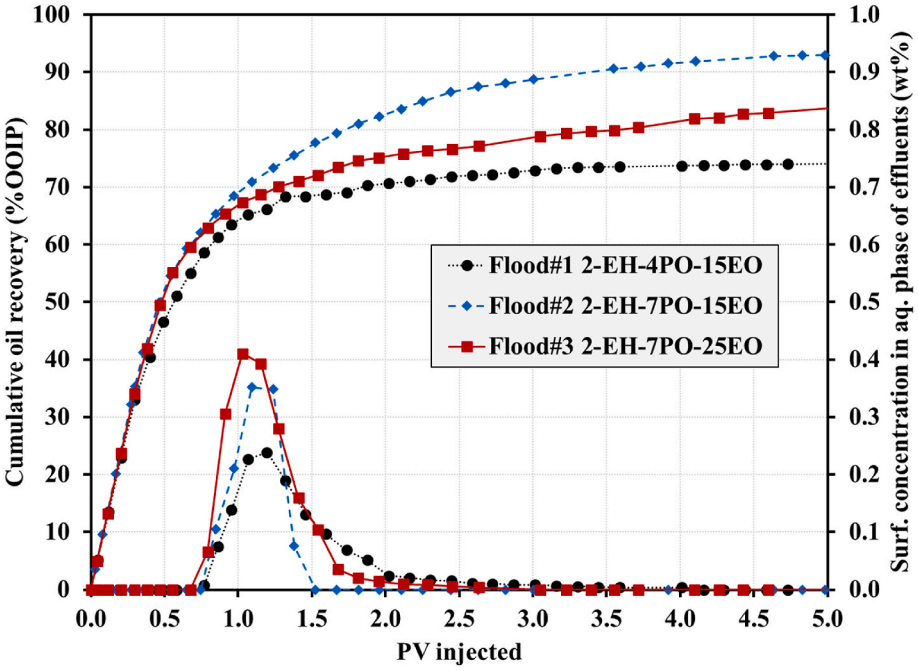

Fig. 9. Comparison of Floods #1, #2, and #3 regarding the cumulative oil recovery and the surfactant concentration in the aqueous phase of effluents.

4. Conclusions

Short-hydrophobe surfactants, 2-EH-4PO-15EO, 2-EH-4PO-25EO, 2-EH-7PO-15EO, and 2-EH-7PO-25EO, were studied for LTP flooding of heavy oil. The main objective of this research was to study the surfactant in-situ propagation and its impact on oil recovery by LTP. In addition to the water/oil IFT, surface adsorption and partition coefficient of the surfactants were measured to analyze the surfactant propagation and retention during the oil displacements. The main conclusions are as follows:

1. The partition coefficient of short-hydrophobe surfactants increased with an increasing PO number or decreasing EO number. For 2-EH-xEO-yEO in this research, the PO group tended to increase the hydrophobicity, reducing the solubility in the aqueous phase. The EO group tended to increase the hydrophilicity, increasing the solubility in the aqueous phase.
2. For each short-hydrophobe surfactant, the partition coefficient decreased with increasing initial surfactant concentration above the CMC for a given temperature, and also decreased with decreasing temperature for a given concentration. This trend of reducing partition coefficient likely comes from the two factors that increase

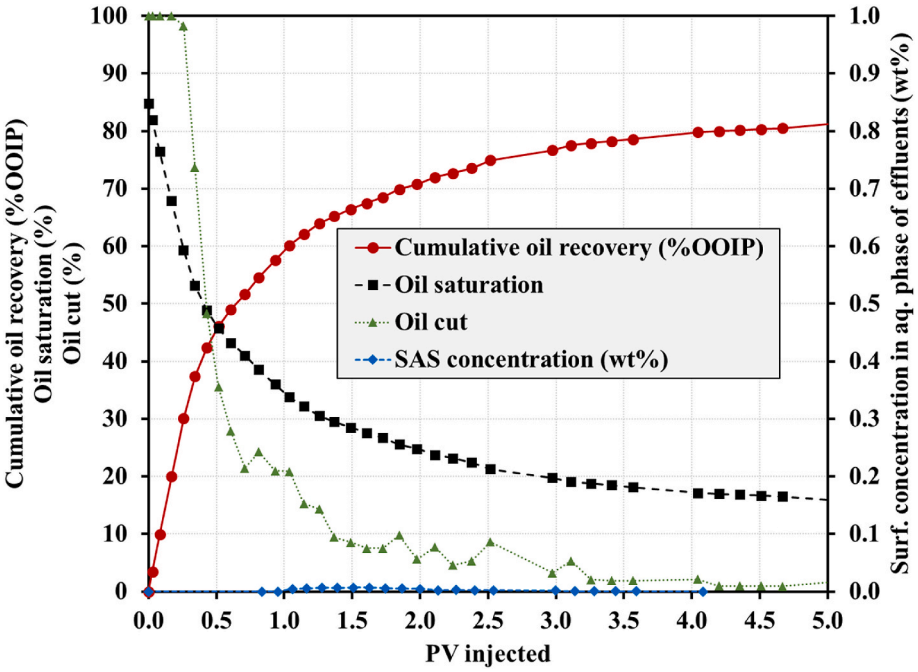

Fig. 10. LTP Flooding Results with a slug of 0.1 wt% 2-EH-7PO-25EO for 0.5 PVI (Flood #4).

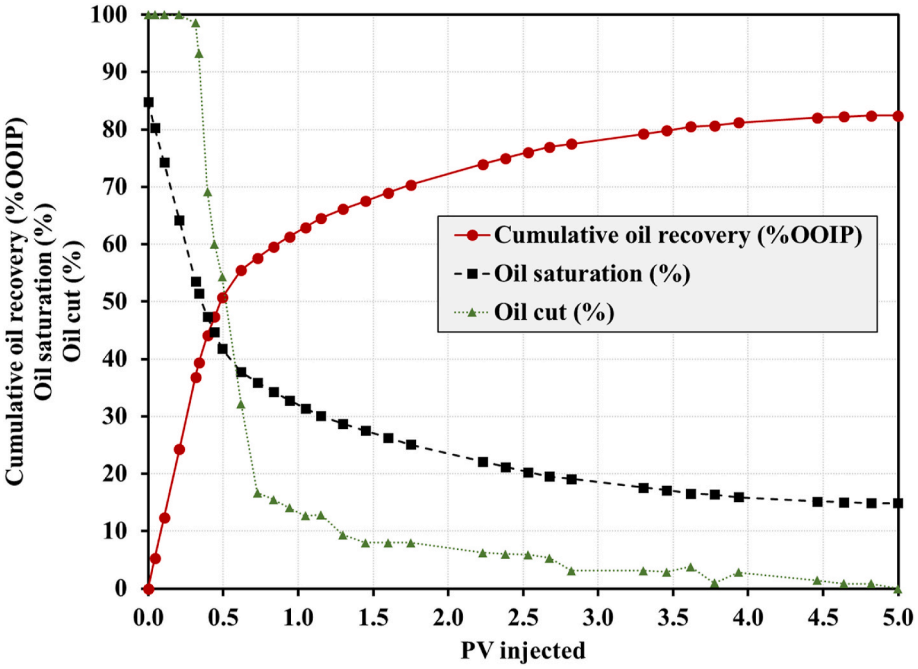

Fig. 11. LTP Flooding Results with a slug of 0.1 wt% 2-EH-7PO-15EO for 0.5 PVI (Flood #5).

the hydrophilicity of the surfactant: a) a greater concentration of the surfactant tends to increase the overall hydrophilicity for a given number of divalent cations in the solution, and b) a greater level of hydrogen bonding in the aqueous phase at lower temperature tends to increase the hydrophilicity.

3. The surface adsorption of 2-EH-xPO-yEO became larger with smaller IFT values. This negative correlation between IFT and adsorption could be explained by the interaction between the hydrophobic group of the surfactant and the grain surface. A surfactant with stronger hydrophobicity could result in higher adsorption on the surface. As a result, 2-EH-7PO-15EO, which has the strongest hydrophobicity among the surfactants tested, gave the greatest adsorption value.
4. When a sufficient amount of surfactant could propagate through the sandpack (i.e., a slug of 0.5 wt% surfactant for 0.5 PVI), the water/oil IFT was the dominant factor for the final oil recovery in the LTP floods. Comparison of 2-EH-4PO-15EO and 2-EH-7PO-25EO for a similar IFT value clearly indicated the importance of the in-situ surfactant propagation in oil displacement. 2-EH-7PO-25EO resulted in greater oil recovery with a lower partition coefficient, although it has a similar IFT value to 2-EH-4PO-15EO.

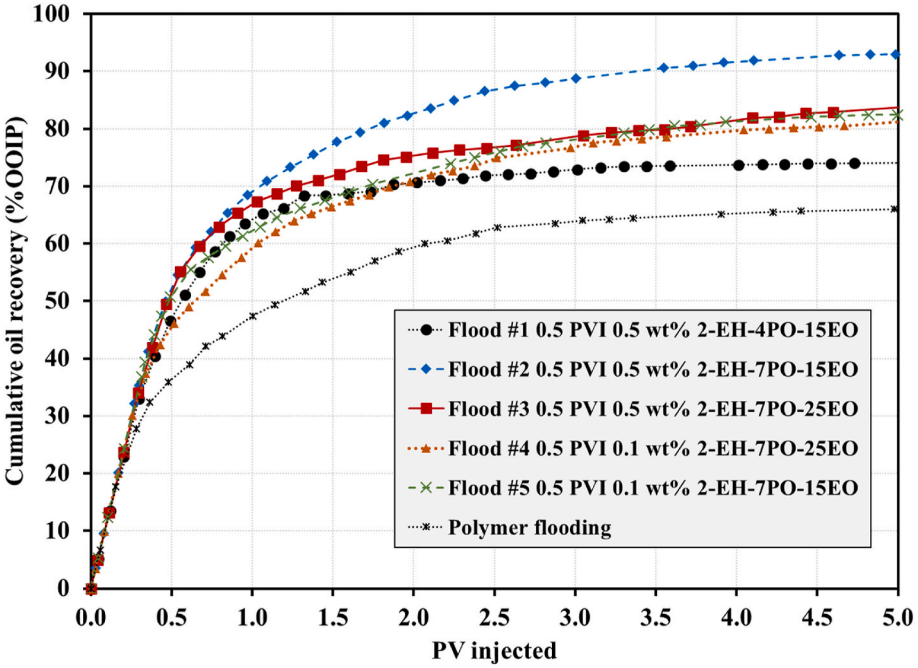

Fig. 12. Comparison of LTP flooding results (Floods #1 - #5). Numerical values for this figure were given in Table 8. The polymer flooding result is shown as a baseline. The polymer flooding data were taken from Baek et al. (2020).

5. With a reduced amount of surfactant (i.e., a slug of 0.1 wt% surfactant for 0.5 PVI), the oil recoveries of Flood #4 (2-EH-7PO-25EO) and Flood #5 (2-EH-7PO-15EO) were essentially the same at the early and late times, although 2-EH-7PO-15EO gave one order of magnitude smaller IFT than 2-EH-7PO-15EO. The analysis of the surfactant propagation indicated that only 2-EH-7PO-25EO propagated through the sandpack with less surfactant loss during the oil displacement (adsorption and trapping in the remaining oil).
6. Results collectively showed that optimization of 2-EH-xPO-yEO for LTP flooding involves two competing factors. One is to minimize the water/oil IFT for increasing the local oil displacement efficiency, and the other is to minimize the partition coefficient for increasing the volumetric sweep efficiency with more efficient in-situ propagation of the surfactant. It is critical to take a balance between these two factors for the surfactant used for LTP flooding.

Credit author statement

Kwang Hoon Baek: Data curation; Formal analysis; Investigation; Methodology; Validation; Visualization; Writing – original draft, Mingyan Liu: Data curation; Investigation; Writing – original draft, Francisco J. Argüelles-Vivas: Data curation; Formal analysis; Investigation; Methodology, Gayan A. Abeykoon: Data curation; Formal analysis; Investigation; Methodology, Ryosuke Okuno: Conceptualization; Formal analysis; Funding acquisition; Investigation; Methodology; Project administration; Resources; Supervision; Validation; Writing – original draft.

Declaration of competing interest

The authors declare that they have no known competing financial interests or personal relationships that could have appeared to influence the work reported in this paper.

Nomenclature

API	American Petroleum Institute
C_S^o	Concentration of surfactant in the oleic phase
C_S^a	Concentration of surfactant in the aqueous phase
CMC	Critical micelle concentration
FR	Filtration ratio
HCl	Hydrochloric acid
HPAM	partially hydrolyzed polyacrylamide
IFT	Interfacial tension
K	Partition coefficient
LTP flooding	Low tension polymer flooding
N_C	Capillary number
S_{oi}	Initial oil saturation
S_{wi}	Surfactant polymer
$CaCl_2{\cdot}2H_2O$	Calcium chloride anhydrate
EO	Ethylene oxide
$MgCl_2{\cdot}6H_2O$	Magnesium chloride hexahydrate

NaCl	Sodium chloride
Na_2SO_4	Sodium sulfate
PO	Propylene oxide
2-EH	2-ethylhexanol
cp	Centipoise
°C	Celsius
g/ml	Gram per milliliter
μm	Micrometer
ppm	Parts per million
psi	Pound per square inch
PV	Pore Volume
PVI	Pore volume injected
OOIP	Original oil in place
wt%	Weight percentage

References

Aitkulov, A., Luo, H., Lu, J., Mohanty, K.K., 2017. Alkali-cosolvent- polymer flooding for viscous oil recovery: 2D evaluation. Energy Fuels 31 (7), 7015–7025. https://doi.org/10.1021/acs.energyfuels.7b00790.

Baek, K.H., Argüelles-Vivas, F.J., Abeykoon, G.A., Okuno, R., Weerasooriya, U.P., 2019. Application of ultrashort hydrophobe surfactants with cosolvent characters for heavy oil recovery. Energy Fuels 33, 8241–8249. https://doi.org/10.1021/acs.energyfuels.9b01716.

Baek, K.H., Argüelles-Vivas, F.J., Abeykoon, G.A., Okuno, R., Weerasooriya, U.P., 2020. Low-tension polymer flooding using a short-hydrophobe surfactant for heavy oil recovery. Energy Fuels 34, 15936–158948. https://doi.org/10.1021/acs.energyfuels.0c02720.

Belhaj, A.F., Elraies, K.A., Alnarabiji, M.S., Shuhli, J.A.B.M., Mahmood, S.M., Ern, L.W., 2019. Experimental investigation of surfactant partitioning in pre-CMC and post-CMC regimes for enhanced oil recovery application. Energies 12, 1–15. https://doi.org/10.3390/en12122319.

Belhaj, A.F., Elraies, K.A., Mahmood, S.M., Zulkifli, N.N., Akbari, S., Hussien, O.S., 2020. The effect of surfactant concentration, salinity, temperature, and pH on surfactant adsorption for chemical enhanced oil recovery: a review. J. Pet. Explor. Prod. Technol. 10, 125–137. https://doi.org/10.1007/s13202-019-0685-y.

Boss, W.F., Mott, R.L., 1980. Effects of divalent cations and polyethylene glycol on the membrane fluidity of protoplast. Plant Physiol. 66 (5), 835–837. https://doi.org/10.1104/pp.66.5.835.

Catanoiu, G., Carey, E., Patil, S.R., Engelskirchen, S., Stubenrauch, C., 2011. Partition coefficients of nonionic surfactants in water/n-alkane systems. J. Colloid Interface Sci. 355, 150–156. https://doi.org/10.1016/j.jcis.2010.12.002.

Ding, L., Wu, Q., Zhang, L., Guérillot, D., 2020. Application of fractional flow theory for analytical modeling of surfactant flooding, polymer flooding, and surfactant/polymer flooding for chemical enhanced oil recovery. Water 12, 2195. https://doi.org/10.3390/w12082195.

Fortenberry, R., Kim, D., Nizamidin, N., Adkins, S., Arachchilage, G., Koh, H.S., Weerasooriya, U.P., Pope, G.A., 2015. Use of cosolvents to improve alkaline/polymer flooding. SPE J. 20, 255–266. https://doi.org/10.2118/166478-PA.

Ghosh, P., Sharma, H., Mohanty, K.K., 2018. Development of surfactant-polymer (SP) processes for high temperature and high salinity carbonate reservoirs. SPE Ann. Tech. Conf. Exhibit. 24 September, 2018, Dallas, Texas, USA. SPE-191733-MS.

Ghoulam, M.B., Moatadid, N., Graciaa, A., Lachaise, J., 2002. Effects of oxyethylene chain length and temperature on partitioning of homogeneous polyoxyethylene nonionic surfactants between water and isooctane. Langmuir 18 (11), 4367–4371. https://doi.org/10.1021/la0117707.

Harwell, J.H., Hoskins, J.C., Schechter, R.S., Wade, W.H., 1985. Pseudophase separation model for surfactant adsorption: isomerically pure surfactants. Langmuir 1 (2), 251–262. https://doi.org/10.1021/la00062a013.

Hirasaki, G.J., 1981. Application of the theory of multicomponenet, multiphase displacemenr to three-component, two-phase surfactant flooding. SPE J. 21, 191–204. https://doi.org/10.2118/8373-PA.

Kalpakci, B., Arf, T.G., Barker, J.W., Krupa, A.S., Morgan, J.C., Neira, R.D., 1990. The Low-Tension Polymer Flood Approach to Cost-Effective Chemical EOR SPE/DOE Enhanced Oil Recovery Symposium, 22-25 April, 1990. Society of Petroleum Engineers, Tulsa, Oklahoma. https://doi.org/10.2118/20220-MS. SPE-20220-MS.

Kamal, M.S., Hussein, I.A., Sultan, A.S., 2017. Review on surfactant flooding: phase behavior, retention, IFT, and field applications. Energy Fuels 31, 7701–7720. https://doi.org/10.1021/acs.energyfuels.7b00353.

Larson, R.G., Hirasaki, G.J., 1978. Analysis of the physical mechanisms in surfactant flooding. SPE J. 42–58 https://doi.org/10.2118/6003-PA.

Maldal, T., Gilje, E., Kristensen, R., Karstad, T., Nordbotten, A., Schilling, B.E.R., Vikane, O., 1998. Evaluation and economical feasibility of polymer-assisted surfactant flooding for the gullfaks field, Norway. SPE Reservoir Eval. Eng. 1, 161–168. https://doi.org/10.2118/35378-PA.

Maltesh, C., Somasundaran, P., 1992. Effect of binding of cations to polyethylene glycol on its interactions with sodium dodecyl sulfate. Langmuir 8 (8). https://doi.org/10.1021/la00044a008, 19301926.

Mannhardt, K., Schramm, L.L., Novosad, J.J., 1992. Adsorption of anionic and amphoteric foam-forming surfactants on different rock types. Colloid. Surface. 68, 37–53. https://doi.org/10.1016/0166-6622(92)80146-S.

Massarweh, O., Abushaikha, A., 2020. The use of surfactants in enhanced oil recovery: a review of recent advances. Energy Rep. 6, 3150–3178. https://doi.org/10.1016/j.egyr.2020.11.009.

Panthi, K., Weerasooriya, U.P., Mohanty, K.K., 2019. Chemical flood of a viscous oil with novel surfactant. In: SPE Annual Technical Conference and Exhibition, 30 September- 2 October, 2019, Calgary, Canada. SPE-196198-MS.

Ravera, F., Ferrari, M., Liggieri, L., Miller, R., Passerone, A., 1997. Measurement of the partition coefficient of surfactants in water/oil systems. Langmuir 13 (18), 4817–4820. https://doi.org/10.1021/la962096+.

Rupprecht, H., Gu, T., 1991. Structure of adsorption layers of ionic surfactants at the solid/liquid interface. Colloid Polym. Sci. 269, 506–522. https://doi.org/10.1007/BF00655889.

Salager, J., Marquez, N., Graciaa, A., Lachaise, J., 2000. Partitioning of ethoxylated octylphenol surfactants in Microemulsion−Oil−Water systems: influence of temperature and relation between partitioning coefficient and physicochemical formulation. Langmuir 16 (13), 5534–5539. https://doi.org/10.1021/la9905517.

Sharma, H., Panthi, K., Mohanty, K.K., 2018. Surfactant-less alkali-cosolvent-polymer floods for an acidic crude oil. Fuel 215, 484–491. https://doi.org/10.1016/j.fuel.2017.11.079.

Shramm, L.L., 2000. Surfactant: Fundamentals and Applications in the Petroleum Industry. Cambridge University Press, ISBN 978-0521157933.

Somasundaran, P., Kunjappu, J.T., 1989. In-situ investigation of adsorbed surfactants and polymers on solids in solution. Colloid. Surface. 37, 245–268. https://doi.org/10.1016/0166-6622(89)80123-4.

Tiberg, F., Joensson, B., Tang, J., Lindman, B., 1994. Ellipsometry studies of the self-assembly of nonionic surfactants at the silica-water interface: equilibrium aspects. Langmuir 10 (7), 2294–2300. https://doi.org/10.1021/la00019a045.

Upamali, K.A.N., Liyanage, P.J., Jang, S.H., Shook, E., Weerasooriya, U.P., Pope, G.A., 2018. New surfactants and cosolvents increase oil recovery and reduce cost. SPE J. 6, 2202–2217. https://doi.org/10.2118/179702-PA.